WARSAW UNIVERSITY OF TECHNOLOGY Index 351733
FACULTY OF CIVIL ENGINEERING
COMMITTEE FOR CIVIL AND WATER ENGINEERING
POLISH ACADEMY OF SCIENCES ISSN 1230-2945

DOI: 10.24425/ace.2023.144158

ARCHIVES OF CIVIL ENGINEERING

Vol. LXIX ISSUE 1 2023

pp. 39 –54

Case study

Influence of the tie reinforcement on the development of a collapse caused by the failure of an edge column in RC flat slab system

Lidia Buda-Ożóg[1], Joanna Zięba[2], Katarzyna Sieńkowska[3], Damian Nykiel[4]

Abstract: RC flat slabs are one of the most popular and effective methods of shaping plates in buildings. Although failures of entire structures are relatively rare, they cannot be excluded from the occupancy cycle of the facility. The research analysis presented in this paper is an attempt to understand more precisely the phenomena that occur in the RC flat slab system and to assess the influence of the additional protection of the flat slabs against progressive collapse in the case of failure of one of the supports. The results were obtained from destructive experimental investigations of a flat reinforced concrete slab made in scale 1:3. The collapse in the analysed model was simulated by removing three edge columns and additional loading by means of hydraulic actuator. In place of the columns removed, differential tie reinforcement was applied. The results obtained confirm that the structure achieved a much higher ultimate load than the one resulting from the design calculations.

Keywords: reinforcement, tie reinforcement, progressive failure, edge column, RC flat slab system, deformation

[1]DSc., PhD., Eng., Department of Building Structures, Faculty of Civil Engineering and Environmental Engineering, Rzeszow University of Technology, Poznańska 2, Rzeszow 35-084, Poland, e-mail: lida@prz.edu.pl, ORCID: 0000-0002-1205-1345

[2]PhD., Eng., Department of Building Structures, Faculty of Civil Engineering and Environmental Engineering, Rzeszow University of Technology, Poznańska 2, Rzeszow 35-084, Poland, e-mail: j.zieba@prz.edu.pl, ORCID: 0000-0003-1800-5697

[3]MSc., Eng., Department of Building Structures, Faculty of Civil Engineering and Environmental Engineering, Rzeszow University of Technology, Poznańska 2, Rzeszow 35-084, Poland, e-mail: k.sienkowska@prz.edu.pl, ORCID: 0000-0003-1497-5821

[4]MSc., Eng., Department of Building Structures, Faculty of Civil Engineering and Environmental Engineering, Rzeszow University of Technology, Poznańska 2, Rzeszow 35-084, Poland, e-mail: d.nykiel@prz.edu.pl, ORCID: 0000-0003-2259-5917

1. Introduction

Reinforced concrete flat slabs are one of the most popular and effective methods of shaping plates in buildings. They are eagerly used by architects because of the possibility of flexible shaping of the space in the building and are easier to manufacture than slab with beams. Flat slab systems are more susceptible to the development of progressive collapse because there are no beams to help redistribute loads in an accident situation [1]. Although failures of entire structures are relatively rare, they cannot be excluded from the occupancy cycle of the facility. Failures may be a consequence of many factors, such as terrorist attacks, uncontrolled impact loads due to road traffic, or human thoughtlessness – especially during the stage of modernization works connected with the change of a facility's function. As has been shown in many works "plasticity of the structure" and especially joints connecting its main elements is the key to prevent or limit the effects of the progressive collapse. On the basis of many studies, reinforced concrete structures, which are characterised by a significant nonlinearity of material and geometric properties, after failure reach a much higher ultimate resistance than obtained from the design calculations. Additionally, elements such as infill walls or slab elements allow the creation of alternative load paths after failure, thus increasing the load capacity of the structure. For this reason, various experimental and numerical studies of flat slabs have been carried out for many years in order to understand the phenomena that occur in the situation of column failure. Some of the first to address the topic of flat slab failures were the work of Hawkins and Mitchell [2] and Mitchell and Cook [3], which focused on experimental studies of such members subjected to extreme loads. It was Mitchell and Cook who recognised the need to design plates so that secondary load-transfer mechanisms could be developed after failure. Extensive experimental investigations on the edge behaviour of slab-column joints and the influence of additional tie beam reinforcement in flat plates were carried out by Starosolski et al. [4,5], Ma [6,7], or Qian and Li [8,9]. The effect of prestressing tie beam reinforcement on the collapse development and failure pattern of a flat slab in a column failure situation was the subject of an experimental study by Yang et al. [10]. On the other hand, Ren [11] and Lu [12] have studied the effect of the type and amount of the main slab reinforcement on its behavior in case of column failure.

The research presented in this paper was aimed at evaluating the behaviour of RC flat slab after edge-column failure depending on the degree and diameter of the applied tying reinforcements. The influence of the location of the removed edge column on the behaviour of the floor after failure was also analysed. Unlike other studies of this type, the real monolithic connection between the slab and the column was taken into account in the research, and the research model was close to the real structural element.

2. Tying system in flat slabs

The methods for preventing accidental or unforeseeable structural failures are divided into two approaches: direct and indirect. The direct approach uses two basic strategies: a strategy based on the determination of the value of exceptional effects and a strategy based

on the limitation of local failure. The second approach, indirect, two methods represents: the key element method or the Alternate Load Path (ALP) method [4]. The key element method involves designing a load-bearing element whose failure causes disproportionate failure or the extent of failure exceeds a specified area to be capable of carrying the design exception load. However, this method is very expensive, as it involves a large excessive size of the structure in unlikely cases. The ALP method allows for the failure of a particular element, but by taking advantage of the additional strength and ductility of the materials used and the increased load carrying capacity resulting from the spatial geometry, it is able to carry much greater loads than designed. The effectiveness of this method depends mainly on properly formed ties connecting the structural elements [13]. This approach is recommended in various design guidelines as a way to increase the resistance of the structure to progressive collapse, e.g. EN 1991-1-7 (2006) [14], UFC 4-023-03 [15], ASCE/SEI 7-16 [16], and IBC 2009 [17]. Depending on the level of risk, the bonding requirements are defined in terms of horizontal or horizontal and vertical elements. In EN 1991-1-7 [14] horizontal ties are required for destruction consequence class CC2a, that is, average risk to human life and significant social and economic consequences. According to EN 1991-1-7 [14] and EN 1992-1-1 [18], horizontal ties must be applied at each storey at floor level in two perpendicular directions to ensure a secure connection between columns and the masonry. These ties shall transfer a minimum tensile force according to the expression:

$$F = 0.8(g + p)l \quad \text{or} \quad 75 \text{ kN} \tag{2.1}$$

where: $g + p$ – the permanent and variable surface action applied on the considered floor, l – the span of the tie.

However, it should be noted that the proposed relationship was derived for the beam nature of the tie elements, assuming a parabolic tendon course with the possibility of rotation at the support by an angle of 32°. Acceptability of such an angle of rotation without prior failure of the concrete in the case of typical flat slab systems is practically impossible. Therefore, in spite of so many articles on the problem of shaping of reinforcement limiting the occurrence of progressive collapse in flat slabs, but being aware of still very approximate idealization of the issue, this subject seems to be still current and not fully understood. This is due to many factors, such as: nonlinearity of material and geometry, effect of scale, compatibility of forming research models in relation to real objects, or the use of modern materials and measurement techniques. The research analysis presented in this paper is an attempt to understand more precisely the phenomena occurring in the RC flat slab system and to assess the influence of the applied additional protection of the flat slabs against the progressive collapse in the case of failure of one of the supports.

3. Experimental design

3.1. Specimen design

The subject of experimental investigations was the 16-field RC flat slab, as shown in Fig. 1. The research included verification of the influence of reinforcement bars made of

B600B steel on the development of progressive collapse caused by the removal of edge support. The purpose of the investigation was to assess defectiveness of the horizontal ties and to observe the changes in the mode of failure of the examined plate fragments depending on the degree and distribution of the B600B steel reinforcement. Geometrically, the test model mirrored the realized 1:3 scale real reinforced concrete flat slab system used in construction. In the test model, the axial spacing of the supports was 2400 mm, resulting in a total slab dimension of 9900 × 9900 mm considering the dimensions of the supports. The test model was supported on 25 square pre-cast columns, 300 × 300 mm in size and 1900 mm in height, articulated to the strength floor. The significant column dimensions adopted, relative to the slab thickness, allowed for the elimination of punching through over a significant spectrum of the anticipated load. Punching shear reinforcement was thus avoided [19]. The plate thickness was selected according to the condition of 1/30 of the floor span between supports, and was 80 mm. Reinforced concrete columns were made in the prefabrication plant, while the remaining part of the monolithic model was made in the Department of the Structure Research of Rzeszow University of Technology. In the conducted analyses, it was assumed that the research model should reflect as closely as possible the real plate in which the plate and the columns are connected monolithically. In order to achieve this effect, reinforcement was released from pre-cast columns and used for monolithic connection with the plate. Above the plate in the place of removed column, a fragment of the column of higher storey was simulated, through which the load was transferred from the actuator. The columns removed in models 1, 2 and 3, respectively, were simulated with easy-to-disassemble slab props – Fig. 2.

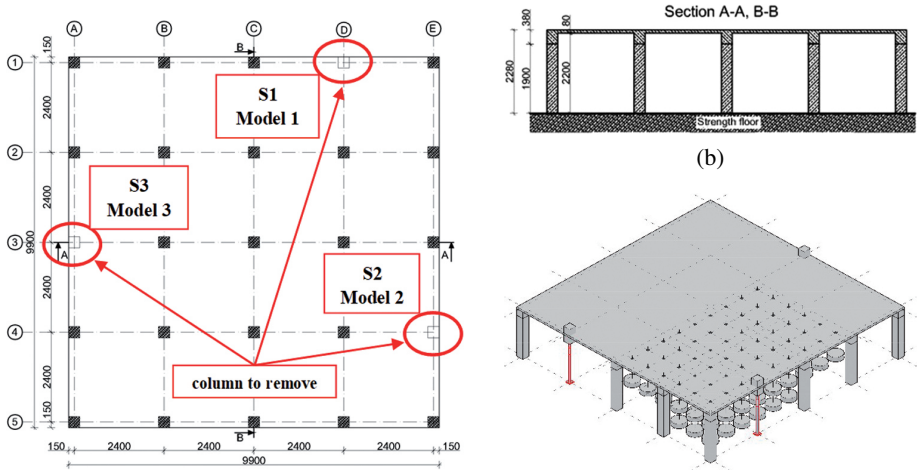

Fig. 1. A simplified view of the model accepted for research: (a) plan view [mm], (b) section A-A, B-B [mm], (c) perspective view

Figure 3 shows the reinforcement of the slab. The bending reinforcement of the slab was made entirely of 10 mm diameter straight bars with 10 mm cover at the bottom and

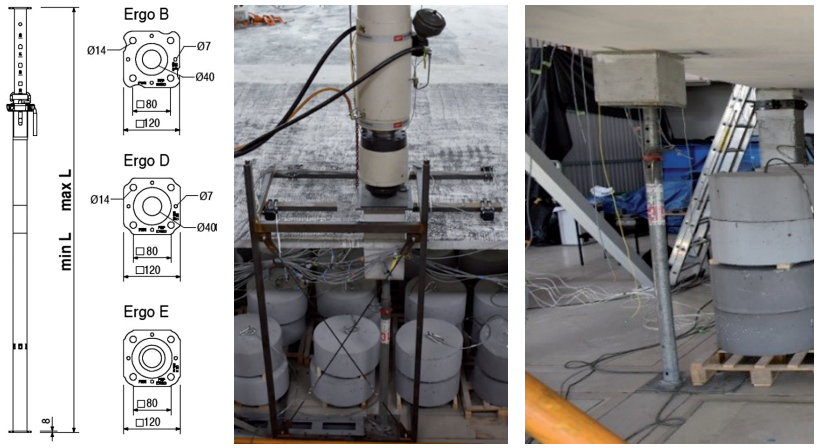

(a) (b)

Fig. 2. View of slab props in place of removed column: (a) slab props scheme, (b) real view of slab props

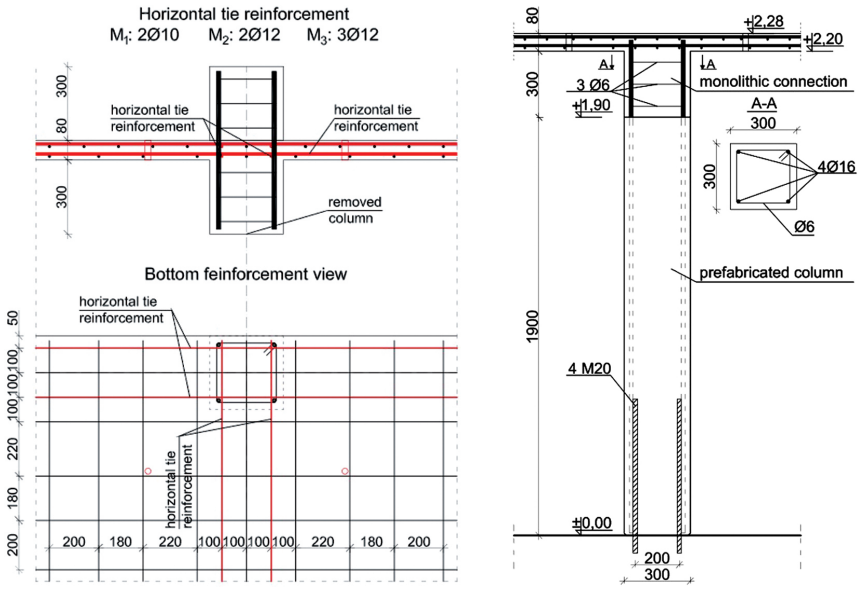

(a) (b)

Fig. 3. View of the reinforcement of the slab and columns

top. The bars of the bottom reinforcement were placed at 200 mm intervals and the top reinforcement over the inner columns at 100 mm intervals and over the perimeter columns at 140 mm intervals. The cross-sectional dimensions of the columns were chosen so that the slab does not require additional punching shear reinforcement. The edges of the slab

are protected with U-shaped bars of 6 mm diameter. The monolithic connection of the slab to the precast reinforced concrete columns was achieved by extending the longitudinal reinforcement bars from the columns to a height of 300 mm and concreting them together with the slab.

3.2. Reinforcement of RC flat plate

Three models with different reinforcements to form the bridging system were considered in the research conducted.

- model 1 (S1 or M1) $\rightarrow 2\phi 10$ As = 157 mm^2,
- model 2 (S2 or M2) $\rightarrow 2\phi 12$ As = 226 mm^2,
- model 3 (S3 or M3) $\rightarrow 3\phi 12$ As = 339 mm^2.

3.3. Material properties

Reinforcing bars with a diameter of 10 mm were used to reinforce the slab, while bars with a diameter of 16 and 12 mm were used to shape the slab-to-column joints and the end reinforcement, respectively. The material parameters of the applied reinforcing steel were determined during the tests according the standard [20] and are summarized in Table 1.

Table 1. Average values of reinforcing bars parameters obtained in tensile tests (56 samples)

Yield strength			Tensile strength			Modulus of elasticity			Strain		
f_{ym}	σ	ν	f_{tm}	σ	ν	E	σ	ν	ε_{uk}	σ	ν
MPa	MPa	%	MPa	MPa	%	GPa	GPa	%	%	%	%
658.1	67.0	10.2	743.2	66.5	8.9	200.5	9.7	4.8	8.7	1.6	18.8

The slab was designed using concrete of class C30/37 of concrete mix consistency S4 and maximum aggregate size of 8 mm. In order to verify the strength parameters of the delivered concrete with the design assumptions, samples were taken for testing during concreting according the standards [21–24]. The mechanical parameters of the concrete obtained during testing are summarized in Table 2 and Table 3.

Table 2. Average compressive strength (6 samples), tensile strength (9 samples) and modulus of elasticity of concrete (3 samples)

The ordered concrete class	Compressive strength			Tensile strength			Modulus of elasticity		
	$f_{\mathrm{cm,\,cube}}$	σ	ν	f_{ctm}	σ	ν	E_{cm}	σ	ν
	[MPa]	[MPa]	[%]	[MPa]	[MPa]	[%]	[GPa]	[GPa]	[%]
C 30/37	57.13	2.08	3.64	4.12	0.22	5.34	39.24	0.99	2.55

Table 3. Average flexural tensile strength of concrete

The ordered concrete class	4-point bending			3-point bending		
	f_{cm}^{flex}	σ	ν	f_{cm}^{flex}	σ	ν
	[MPa]	[MPa]	[%]	[MPa]	[MPa]	[%]
C 30/37	7.26	0.25	3.51	8.01	0.58	7.26

3.4. Test set-up and procedure

The loading of each separated research model was divided into two main stages. In the first stage, gravity loading was progressively implemented to represent the assumed permanent and variable actions on the plate. To simulate these actions, 200 kg and 100 kg were used, distributed in such a way that maximum values of internal forces were generated in the slab in the area of the removed column – Fig. 4a. The weights were suspended at 54 or 72 points on the 800 × 800 mm grid, depending on the model. After suspending all assumed gravity loads, in the next step, the catastrophe caused by the removal of the edge support was simulated. Under full gravity loading, the support was removed at the column location, and the possible forces in the real object at the damaged column location were simulated using a hydraulic actuator – Fig. 4b. The concentrated load was implemented in steps of 5 kN until failure, using an Instron-Schenck actuator.

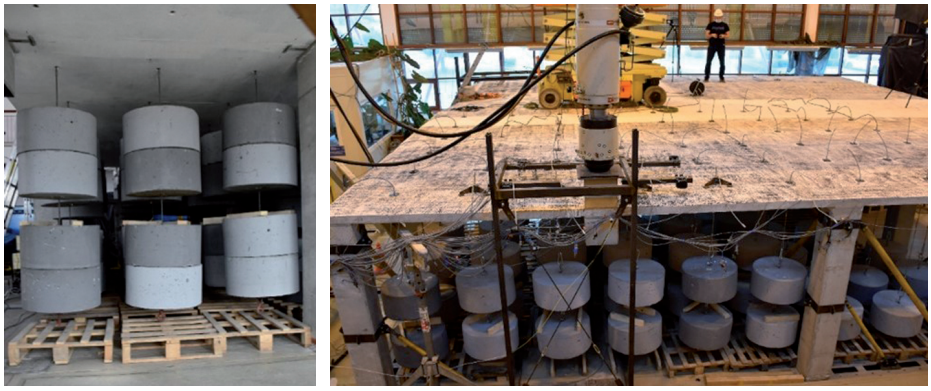

(a) (b)

Fig. 4. Plate loading: (a) view of weights used for gravity loading, (b) loading after removal of support – gravity and hydraulic simultaneously

In order to measure displacement, an inductive and drawn wire sensor was used. The sensors are installed on specially designed support structures – Fig. 5a. The sensor layout was planned every time in the two fields of the most affected slab area. In order to measure the displacements of the plate, the ARAMIS [25–27] optical image correlation system, developed by the German company GOM, was also used – Fig. 5b. The system used in this study was a system of two cameras, with a focal length of 17 mm and a shooting speed of

12 Hz with a resolution of 1600 × 1200 pixels, that is 1.92 Mpix. The dimension of the measurement space was 3840 × 3065 mm. The plate displacement in the fields adjacent to the mainly loaded fields was measured using a conventional total station. The measurement set consisted of eight prisms and a Leica total station, Fig. 5c.

(a) (b) (c)

Fig. 5. Methods of displacement measurement used: (a) ARAMIS system, (b) displacement transducer and draw-wire sensor, (c) Leica TS60 total station +8 prisms

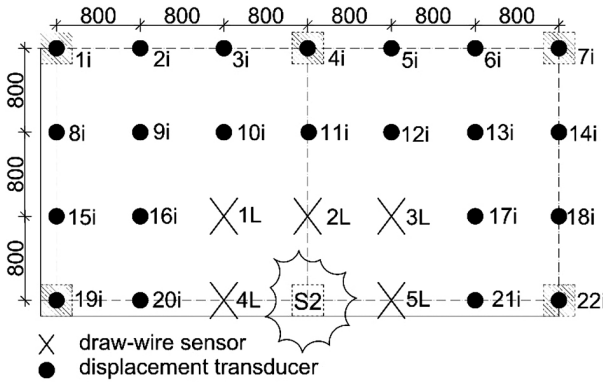

Fig. 6. Example of draw-wire sensors and displacement transducers placement at one of the removed columns

During the tests conducted, strain gauges and fiber optic strain sensors were used to measure strain. In the tested element, 76 electrofusion strain gauges TFs 5/120 were stuck on the reinforcing steel – Fig. 7a and 36 strain gauges TFs 60/120 on the concrete – Fig. 7b. The distribution of the strain gauges was designed in areas adjacent to the removed supports. Fiber optic strain sensors were also used to measure strain, allowing quasicontinuous measurements along the length of a single fiber at 1 cm spacing. The fiber optic sensors were placed along the reinforcing bars of the bottom rim reinforcement – Fig. 7c.

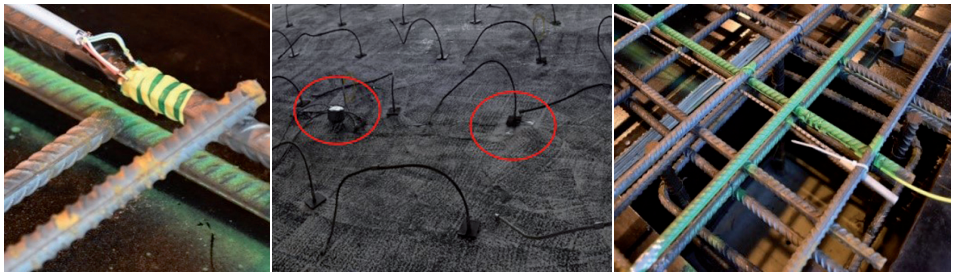

(a) (b) (c)

Fig. 7. Strain measurement methods used: (a) strain gauges on reinforcing steel, (b) strain gauges on concrete, (c) fiber optics on reinforcing bar

4. Results of experimental test

Experimental tests, which are the subject of this paper, were carried out for three days, during which particular models of structure reinforcement were considered and the corresponding supports were removed. Fig. 8 shows examples of photographs from the research. In the gravity loading step, all three models analysed were loaded in the same way, i.e. with concrete weights. In the next step of the investigation, after removing the support, the load was realized using a hydraulic system.

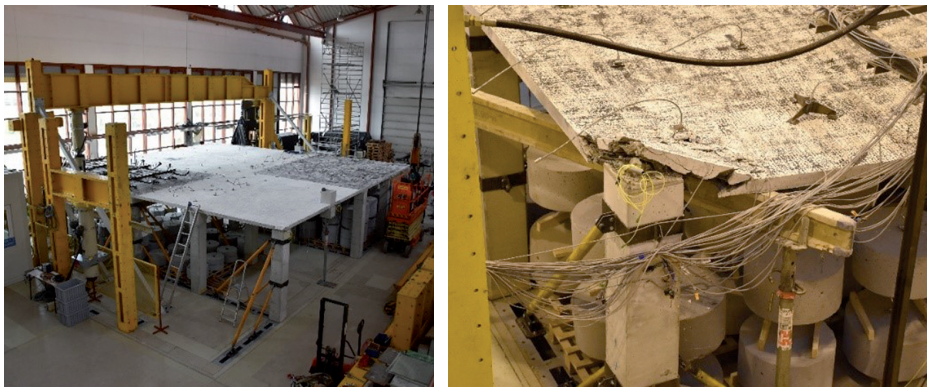

(a) (b)

Fig. 8. Examples of pictures from the implementation of experimental tests

Depending on the reinforcement in horizontal ties (reinforcement model), different values of the maximum load were achieved, which was defined as the ultimate load. The key location for the analysis of the plate was the location of the support removal, so first the vertical displacement values of the plate at the location of the support loss were plotted as a function of the realised loads, with the failure load highlighted – Fig. 9.

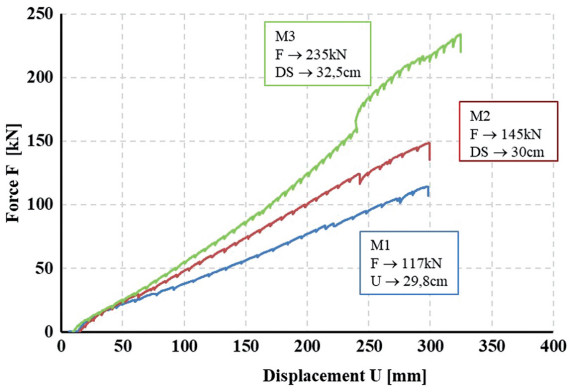

(a)

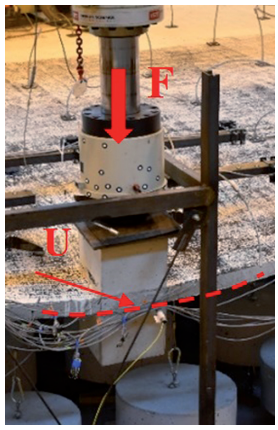

(b)

Fig. 9. Diagram of vertical displacements in the place of removed support as a function of load for tested models

The displacement measurement sensors used in the experimental study determined the lines along which the vertical displacements of the top surface of the plate of each model are shown. As an example, plots of vertical displacement along the edge determined by the sensors marked as 20i, 4L, 5L and 21i, i.e. the extreme edge, are shown in Fig. 10 (location shown in Fig. 6). The initial displacement in the graph was caused by removing the support before the force began.

Based on displacement measurements described in 3.4, diagrams were prepared showing the deformation of the upper surface of the tested plate as a function of the realised loads – Fig. 11.

Fig. 12 shows the scale of destruction of the supports adjacent to the removed column. The approximate angle of rotation at both supports adjacent to the removed column is indicated in the presented figures. The rotation angles were estimated based on the values of plate surface displacements obtained from differential inductance sensors and displacement maps from the Aramis system. The values of the plate rotation angles at the supports shown in Fig. 12 are relatively small and deviate significantly from the assumption of a parabolic tendon course after column failure and an assumed rotation angle at the support of about 32°.

The results obtained confirmed the high sensitivity of the electrofusion strain gauges to work in a complex state of stress and many measurement results were rejected as erroneous and unreliable. It was also observed that most electrofusion strain gauges failed when the reinforcing steel reached its yield point. Figure 13 compares an example of measured strains of tie bottom reinforcement obtained from strain gauges taped at the centre of the span between the column being removed and the adjacent column.

The most information about the behavior of reinforcements during the research was provided by measurements made with fiber optic sensors. Based on the measurements it is possible to determine the area of the strain changes of tested bars and, what is most

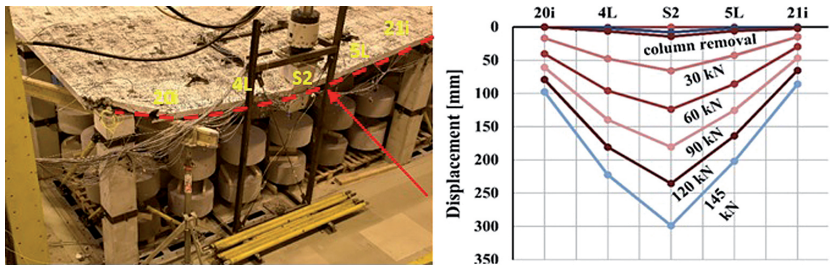

(a) M1

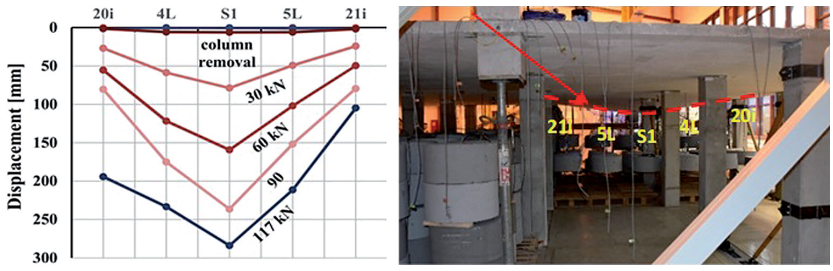

(b) M2

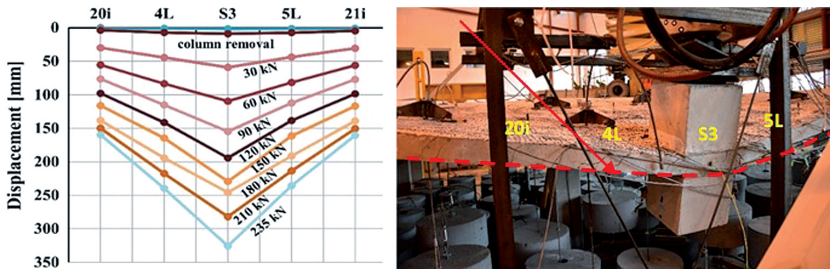

(c) M3

Fig. 10. Vertical displacement along the extreme edge of the plate along with examples of experimental photographs: (a) M1, (b) M2, (c) M3

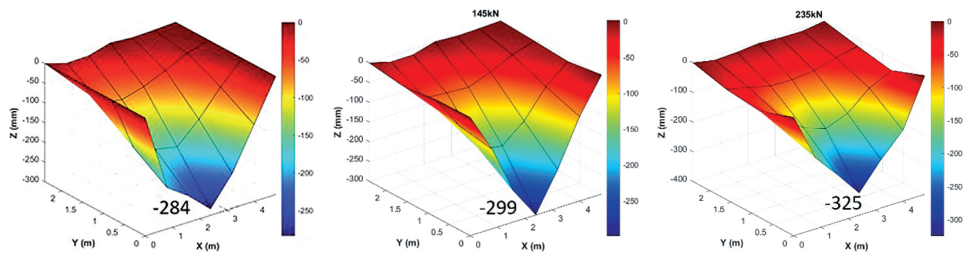

(a) M1 (b) M2 (c) M3

Fig. 11. Deformation maps of the top plate surface of models for the maximum load reached: (a) M1 F = 117 kN, (b) M2 F = 145 kN, (c) M3 F = 235 kN

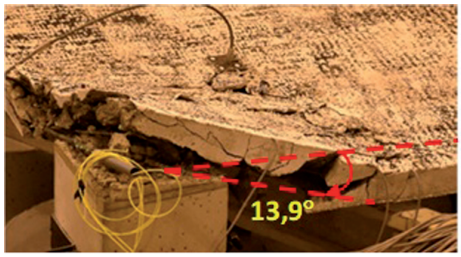

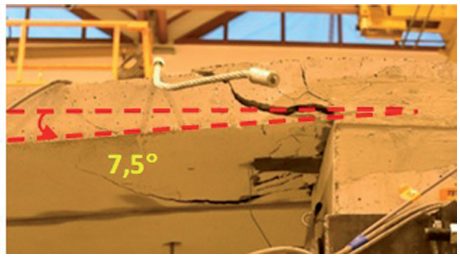

(a) M1 left support right support

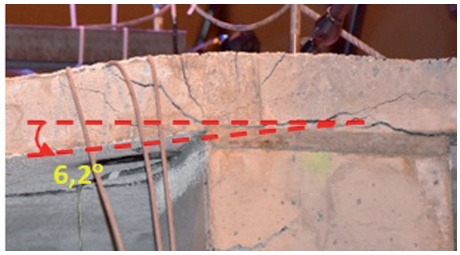

(b) M2 left support right support

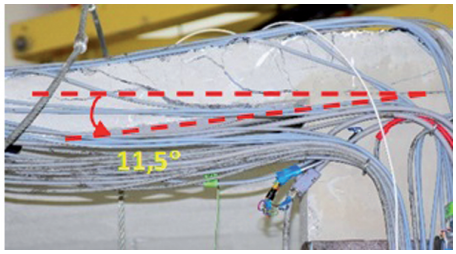

(c) M3 left support right support

Fig. 12. Strain of reinforcing steel: (a), (b) diagrams of change of deformation of selected points on bars of bottom reinforcement in area of removed column, (c) diagram of location of strain gauges on bottom reinforcement

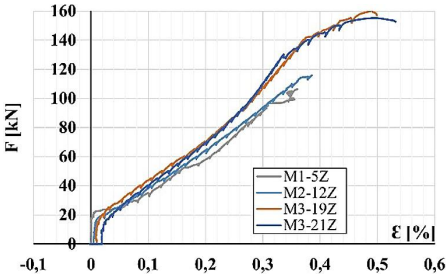

(a)

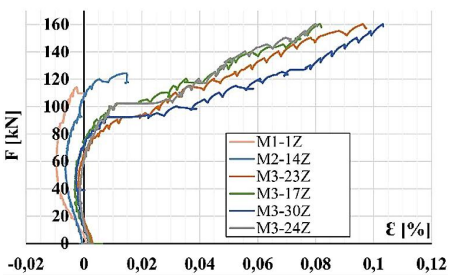

(b)

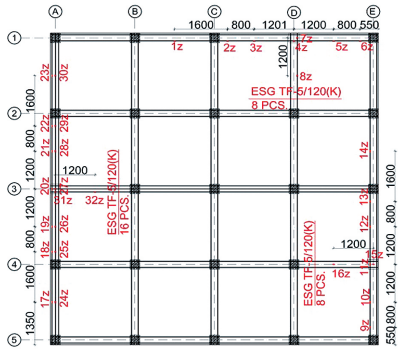

(c)

Fig. 13. Strain of reinforcing steel: (a), (b) diagrams of change of deformation of selected points on bars of bottom reinforcement in area of removed column, (c) diagram of location of strain gauges on bottom reinforcement

important, these strain gauges showed higher resistance to work in the complex stress state. However, some of the strain gauges were destroyed during the execution of the plate. Fig. 14 shows the maximum strain of the bottom reinforcement added due to the progressive collapse obtained from the fiber optic sensors for model 1 and model 2. On the M3 model, unfortunately all the wire sensors were destroyed and results could not be generated.

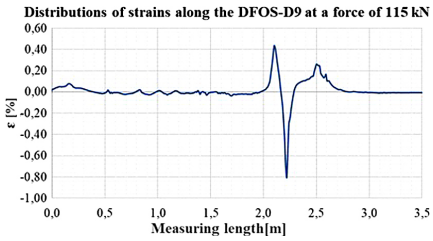

(a) M1 – D9

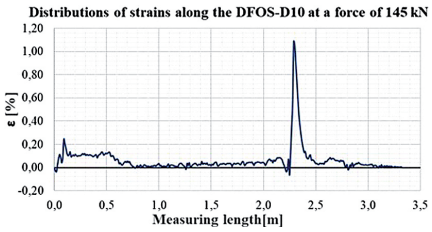

(b) M2 – D2

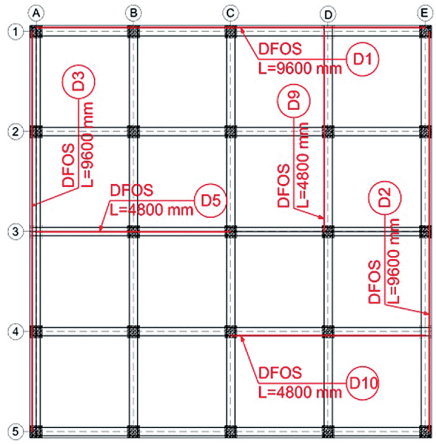

(c)

Fig. 14. Strains distribution on bars of the bottom reinforcement perpendicular to the removed column in models M1 and M2 for maximum load: (a) diagram for M1, (b) diagram for M2, (c) diagram of sensor locations

As shown in Figure 14, the measured member strains are local and reach their maximum values over the removed column at the point where the concentrated load is applied. The range of observed significant changes in deformation of reinforcement did not exceed the band of 50 cm.

5. Conclusions

On the basis of the conducted experimental tests and obtained results, it was noted:

- The deformation of the flat slab edge in case of column losse is much smaller than the deformation which is the basis for determining the tensile force in ties formula 2.1. For the monolithic connection of the slab and column reinforcement, the floor deformation recommended in the standard (32 degrees) was not possible to achieve.
- By comparing the results of these models (M1, M2 I M3) it is noted that the post-failure capacity of the floor depends not only on the ties reinforcement but also on the degree of flat slab system.
- Comparing model M1 and M2, one can see the key role of the floor slab in the way the structure behaves and resists due to support failure. As shown in the study, increasing the area of the rim reinforcement by 43% resulted in an increase in the failure load by only 23%. Taking into account after the failure of the column the beneficial influence of the alloy plate, i.e. the area of the plate reinforcement in the area separated by the hinge lines, it can be assumed that the total change of the area of reinforcement in Model M2 in comparison to Model M1 is much smaller and amounts to about 11%.
- As the conducted research showed, the location of the removed support is also very important in the assessment of the structure resistance. In case of M3 model, 62% increase of load in relation to M2 model was observed, while the area of the ring reinforcement was increased by 50%.

The research confirmed the observations of other authors of similar research papers [6] concerning the important role of yaks and the need of appropriate shaping and anchoring of the ring reinforcement. As shown in the photographs of floor failure – Fig. 10a and 10b, in case of failure columns in model M1, M2, the coronary reinforcement should be connected with the corner column reinforcement. However, it has to be considered that in real objects there is a continuation of the corner column, so the failure pattern above the outermost support may be different. The investigations carried out showed that in case of monolithic connection between the slab and the column, the assumptions made in the nom. to determine the minimum values of the tensile force deviate from the results obtained. The tensile forces obtained from the tests are significantly greater than those determined from the standard analytical formulas. The reason for this may be both different deformation of the system than assumed in the standard and distinct influence of the floor slab. Deeper understanding of this problem, however, requires further research on similar real models, but including columns above the analysed floor.

References

[1] P. Foraboschi, "Structural layout that takes full advantage of the capabilities and opportunities afforded by two-way RC floors, coupled with the selection of the best technique, to avoid serviceability failures", *Engineering Failure Analysis*, vol. 70, pp. 387–418, 2016, DOI: 10.1016/j.engfailanal.2016.09.010.

[2] N.M. Hawkins and D. Mitchell, "Progressive Collapse of Flat-Plate Structures", *Journal of the American Concrete Institute*, vol. 76, no. 7, pp. 775–808, 1979.

[3] D. Mitchell and W. D. Cook, "Preventing Progressive Collapse of Slab Structures", *Journal of Structural Engineering*, vol. 110, no. 7, pp. 1513–1532, 1984, DOI: 10.1061/(ASCE)0733-9445(1984)110:7(1513).

[4] W. Starosolski, B. Wieczorek, and M. Wieczorek, *Konstrukcje płytowo-słupowe. Zabezpieczenia przeciwko katastrofie postępującej. Biuletyn Techniczny nr 6*. Centrum Promocji Jakości Stali, 2015.

[5] B. Wieczorek, M. Wieczorek, and W. Starosolski, *Badania zachowania się krawędziowych połączeń płyta-słup zbrojonych stalą EPSTAL o wysokiej ciągliwości w stadium awaryjnym wywołanym przebiciem. Biuletyn Techniczny nr 8*. Centrum Promocji Jakości Stali, 2017.

[6] F. Ma, B.P. Gilbert, H. Guan, H. Xue, X. Lu, and Y. Li, "Experimental study on the progressive collapse behaviour of RC flat plate substructures subjected to corner column removal scenarios", *Engineering Structures*, vol. 180, pp. 728–741, 2019, DOI: 10.1016/j.engstruct.2018.11.043.

[7] F. Ma, B.P. Gilbert, H. Guan, H. Xue, X. Lu, and Y. Li, "Experimental study on the progressive collapse behaviour of RC flat plate substructures subjected to edge-column and edge-interior-column removal scenarios", *Engineering Structures*, vol. 209, art. no. 110299, 2020, DOI: 10.1016/j.engstruct.2020.110299.

[8] K. Qian and B. Li, "Experimental study of drop-panel effects on response of reinforced concrete flat slabs after loss of corner column", *ACI Structural Journal*, vol. 110, no. 2, pp. 319–329, 2013.

[9] K. Qian and B. Li, "Resilience of flat slab structures in different phases of progressive collapse", *ACI Structural Journal*, vol. 113, no. 3, pp. 537–548, 2015, DOI: 10.14359/51688619.

[10] T. Yang, Z. Liu, and J. Lian, "Progressive collapse of RC flat slab substructures with unbonded posttensioning strands after the loss of an exterior column", *Engineering Structures*, vol. 234, pp. 1–12, 2021, DOI: 10.1016/j.engstruct.2021.111989.

[11] P.Q. Ren, Y. Li, X.Z. Lu, H. Guan, and Y. L. Zhou, "Experimental investigation of progressive collapse resistance of one-way reinforced concrete beam–slab substructures under a middle-column-removal scenario", *Engineering Structures,* vol. 118, pp. 28–40, 2016, DOI: 10.1016/j.engstruct.2016.03.051.

[12] X.Z. Lu, K.Q. Lin, Y. Li, H. Guan, P.Q. Ren, and Y.L. Zhou, "Experimental investigation of RC beam-slab substructures against progressive collapse subject to an edge-column removal scenario", *Engineering Structures*, vol. 149, pp. 91–103, 2017, DOI: 10.1016/j.engstruct.2016.07.039.

[13] U. Starossek, *Progressive Collapse of Structures*, 2nd ed. Thomas Telford Publishing, 2017.

[14] EN-1991-1-7:2008 Actions on structures – Part 1–7: General actions – Accidental actions.

[15] UFC 04-023-03: Unified facilities criteria: Design of buildings to resist progressive collapse, with change 3 (No. UFC 04-023-03). United States Department of Defense, Washington (DC), US.

[16] *Minimum Design Loads and Associated Criteria for Buildings and Other Structures: ASCE/SEI 7-16*. Reston, USA: American Society of Civil Engineers, 2017.

[17] International Building Code (IBC). International Code Council, 2018.

[18] EN-1992-1-1:2008 Eurocode 2: Design of concrete structures – Part 1-1: General rules and rules for buildings.

[19] T. Urban, M. Gołdyn, and Ł. Krawczyk, "Strengthening of RC slabs against punching shear in theory and practice", *Archives of Civil Engineering*, vol. 67, pp. 317–335, 2021, DOI: 10.24425/ace.2021.138502.

[20] ISO 15630-1:2019 Steel for the reinforcement and prestressing of concrete – Test methods – Part 1: Reinforcing bars, rods and wire.

[21] PN-EN 12390-3:2019-07 Badania betonu. Część 3: Wytrzymałość na ściskanie próbek do badań.

[22] PN-EN 12390-6:2019-08 Badania betonu. Część 5: Wytrzymałość na zginanie próbek do badań.

[23] PN-EN 12390-6:2011 Badania betonu. Część 6: Wytrzymałość na rozciąganie przy rozłupywaniu próbek do badań.

[24] PN-EN 12390-13:2021-12 Badania betonu. Część 13: Wyznaczenie siecznego modułu sprężystości przy ściskaniu.

[25] K. Urbańska, "Zastosowanie systemu ARAMIS do pomiarów odkształceń konstrukcji murowych", *Zeszyty Naukowe Uniwersytetu Zielonogórskiego*, vol. 166, 2017.

[26] C. Ajdukiewicz, M. Gajewski, and P. Mossakowski, "Zastosowanie systemu optycznej korelacji obrazu "ARAMIS" do identyfikacji rys w elementach betonowych", *Logistyka,* vol. 6, pp. 27–34, 2010.

[27] M. Malesa, K. Malowany, U. Tomczak, B. Siwek, M. Kujawińska, and A. Siemińska-Lewandowska, "Application of 3D digital image correlation in maintenance and process control in industry", *Computers in Industry*, vol. 64, no. 9, pp. 1301–1315, 2013, DOI: 10.1016/j.compind.2013.03.012.

Wpływ zbrojenia wieńcowego na rozwój katastrofy spowodowanej awarią słupa krawędziowego w ustroju płytowo-słupowym

Słowa kluczowe: zbrojenie, zbrojenie wieńcowe, zniszczenie postępujące, słup krawędziowy, strop słupowo-płytowy, odkształcenie

Streszczenie:

Układy słupowo-płytowe są jedną z najbardziej popularnych i efektywnych metod kształtowania płyt w budynkach. Mimo że awarie całych konstrukcji zdarzają się stosunkowo rzadko, nie można ich wykluczyć z cyklu użytkowania obiektu. Przedstawione w niniejszej pracy analizy badawcze są próbą dokładniejszego zrozumienia zjawisk zachodzących w układzie płaskich płyt żelbetowych oraz oceny wpływu zastosowanego dodatkowego zbrojenia płyt przed postępującym zawaleniem w przypadku zniszczenia jednej z podpór. Wyniki uzyskano na podstawie niszczących badań doświadczalnych stropu żelbetowego wykonanego w skali 1:3. W analizowanym modelu symulowano zawalenie się stropu poprzez usunięcie trzech słupów krawędziowych i dodatkowe obciążenie siłownikiem hydraulicznym. W miejsce usuniętych słupów zastosowano zróżnicowane zbrojenie cięgnowe. Uzyskane wyniki potwierdzają, że konstrukcja osiągnęła znacznie większe obciążenie granicznie nośne niż to, które wynikało z obliczeń projektowych.

Received: 2022-03-17, Revised: 2022-06-28